Weed location and recognition based on UAV imaging and deep learning

Rufei Zhang[1,2], Cong Wang[1,2], Xiaoping Hu[3,4], Yixue Liu[1,2], Shan Chen[1,2], Baofeng Su[1,2*]

(1. *College of Mechanical and Electronic Engineering, Northwest A&F University, Yangling, Shaanxi, 712100, China*;
2. *Key Laboratory of Agricultural Internet of Things, Ministry of Agriculture and Rural Affairs, Yangling, Shaanxi, 712100, China*;
3. *State Key Laboratory of Crop Stress Biology for Arid Areas, Yangling, Shaanxi, 712100, China*;
4. *College of Plant Protection, Northwest A&F University, Yangling, Shaanxi, 712100, China*)

Abstract: To locate and identify weeds in a wheat field efficiently, an unmanned aerial vehicle (UAV) based imaging method was developed in this study. A weed detection model based on image data through deep learning was developed and implemented. The model uses the YOLOV3-tiny network to detect the pixel coordinates of weeds in images. It acquires the position of weeds by converting the pixel coordinates to the geodetic coordinates. The identified weeds were marked on the prescription map. The algorithm was implemented and tested using a commercial DJI Phantom 3 UAV. This study tested the performance of YOLOV3 and YOLOV3-tiny and found that YOLOV3-tiny was more suitable for mobile devices. The performance of YOLOV3-tiny at different thresholds was tested. The test results show that the model performs optimally when the threshold of the YOLOV3-tiny network is 0.5, under this condition, the mean Average Precision (mAP) is 72.5%, the Intersection-over-Union (IOU) is 80.12%, and the mobile device processing speed is 2FPS. After testing and analyzing weed positioning, results show the average positioning error is 10.31 cm, which is extremely small in agricultural operations. The UAV-based weed position detection system can locate and identify weeds in the crop field at a high speed, efficiently and effectively.

Keywords: UAV, deep learning, weed location, weed recognition, imaging method, target detection, Android APP
DOI: 10.33440/j.ijpaa.20200301.63

Citation: Zhang R F, Wang C, Hu X P, Liu Y X, Chen S, Su B F. Weed location and recognition based on UAV imaging and deep learning. Int J Precis Agric Aviat, 2020; 3(1): 23–29.

1 Introduction

The distribution of weeds in a crop field is mostly disordered, which results in spraying weeds in crop field takes a lot of time and manpower, therefore, it is extremely important to monitor the position of weeds in real-time to provide decision support for weeding. By determining the location and type of field weeds, then applying quantitative herbicide chemicals to these areas for precise spraying, the total amount of herbicide chemicals used can be greatly reduced[1], thereby limiting input costs and environmental losses[2]. When mapping weeds in fields, the appropriate data acquisition and processing platform is the primary issue. Weed detection and image processing can be performed on different platforms[3].

The lack of robust weed sensing technology is the main limitation for developing commercial robotic systems[4]. Milioto et al.[9] proposes a system that combines vegetation detection and deep learning to obtain a high-quality classification of the vegetation in the field into value crops and weeds. Potena et al.[10] presents a perception system for agriculture robotics that enables an unmanned ground vehicle (UGV) equipped with a multispectral camera to automatically perform the weed detection and classification tasks in real-time. However, for the large field, these systems cannot provide high efficiency and quick weeds detection.

UAVs have been proposed as promising tools in several agricultural applications, for providing spatial data with a low-cost autopilot system[5]. The limited computing resources in current UAV systems cannot support the requirements of real-time weeds detection[8], therefore, very few studies focus on the real-time identification of crop field weeds by UAV. However, the relatively powerful computing performance of the drone control terminal provides the possibility for real-time weed differentiation, as well as the weed distribution over a wide range.

In terms of weeds detection, deep learning provides high accuracy in classification and detection, outperforming existing commonly used image processing techniques[6,7]. Therefore, combining the UAV techniques with deep learning methods may provide an effective solution for detecting the distribution of the weed in a large field timely.

To quickly and accurately locate weeds in crop fields, this study developed a real-time weed detection system based on UAV. Firstly, to adapt to the computing performance of the control end, an improved deep learning network was developed for weed identification and localization; then, an Android-based drone control application was developed. This App implements basic drone start-stop control, track planning, and other functions while embedding a weed real-time detection algorithm, which can realize real-time processing of returned images. The system realizes real-time detections of crop field weeds and displays them in the

Received date: 2020-02-10 **Accepted date:** 2020-03-16
Biography: Rufei Zhang, Postgraduate student, research interests: remote sensing in agricultural monitoring direction, Email: 2017052028@ nwafu.edu.cn; **Cong Wang,** Postgraduate student, research interests: application of UAV in agricultural, Email: wangcong19950428@nwafu.edu.cn; **Xiaoping Hu,** PhD, research interests: plant Disease, Email: xphu@nwsuaf.edu.cn; **Yixue Liu,** Postgraduate student, research interests: field plant phenotyping analysis, Email: sunnyliu@nwafu.edu.cn; **Shan Chen,** Postgraduate student, research interests: plant protection, Email: 1791367653@qq.com

*** Corresponding author: Baofeng Su,** PhD, research interests: agricultural remote sensing technology and intelligent detection. Email: bfs@nwsuaf.edu.cn

terminal, and saves the generated prescription maps to the terminal for convenient viewing, thereby providing accurate weeds position information for plant protection UAV.

2 Materials and methods

2.1 Experimental site

The experimental site is located at the experimental farm of Northwest A&F University, Yangling, Shaanxi Province (34°18'18.02"N, 108°5'40.77"E). Crops grown in the study area are winter wheat, and there are mainly 5 kinds of weeds distributed unevenly in crop fields as shown in Figure 1.

2.2 Data acquisition

To ensure the universality of this research, the mobile operating system selected Android, which is the mobile system with the most users. Android is an open-source mobile operating system based on the Linux kernel. The Open Handset Alliance (OHA), established by Google, primarily for touchscreen mobile devices such as smartphones and other portable devices. The UAV selected the DJI phantom 3, which is one of the commonly used UAV equipped with a built-in GPS receiver to obtain the UAV latitude and longitude information. The GPS mode of phantom 3 is GPS/GLONASS, the lens is FOV94°20 mm, f/2.8, and the effective pixel is 12 million.

The UAV was used to collect low-altitude remote sensing data in March 2018. The flight altitude was maintained at 2 meters during the experiment. 2000 original images were collected, 1600 of them are used to train the model and the other parts are used to verify the model.

Cirsium Setosum Descurainia Sophia Euphorbia Helioscopia Veronica Didyma Avena Fatu

Figure 1 Different weeds in the study area

2.3 Weed detection method

Increasing numbers of studies on running deep learning models on mobile devices with limited computing power and memory resource encourages have been processed. Several efficient architectures have been proposed in recent years, for example, MobileNet[11] and ShuffleNet[12]. However, all these models are heavily dependent on depthwise separable convolution which lacks efficient implementation in most deep learning frameworks[13].

YOLO[14] frame object detection as a regression problem, separating the bounding boxes of space and associated class probabilities. A single neural network predicts bounding boxes and class probabilities directly from the complete image in one evaluation. The principle of YOLO detection process is shown in Figure 2. YOLO model processes images in real-time at 45 frames per second. That is to say, YOLO can perform real-time processing on the video on the host. The improved algorithm of the YOLO, YOLOV2[15] and YOLOV3[16], has been proposed to further improve the detection speed.

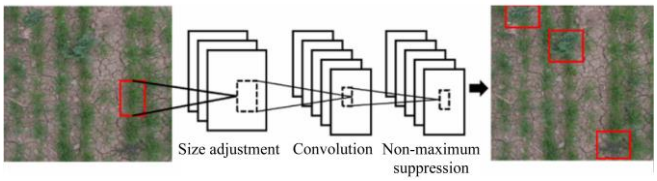

Figure 2 Detection process of YOLO

The network structure of YOLOV3 is shown in Figure 3. The backbone network is the residual layer of darknet53. It uses convolution with a step size of 2 for downsampling instead of the pooling layer. The branch network is the predicted output of 3 different scales.

YOLOV3-tiny is a lightweight version of YOLOV3, taking into account the detection speed and accuracy, reducing the amount of model calculation. The network structure of YOLOV3-tiny is shown in Figure 4. This study selected the Darknet neural network framework for training and testing[17], get a lightweight detection system that can be used on the mobile side.

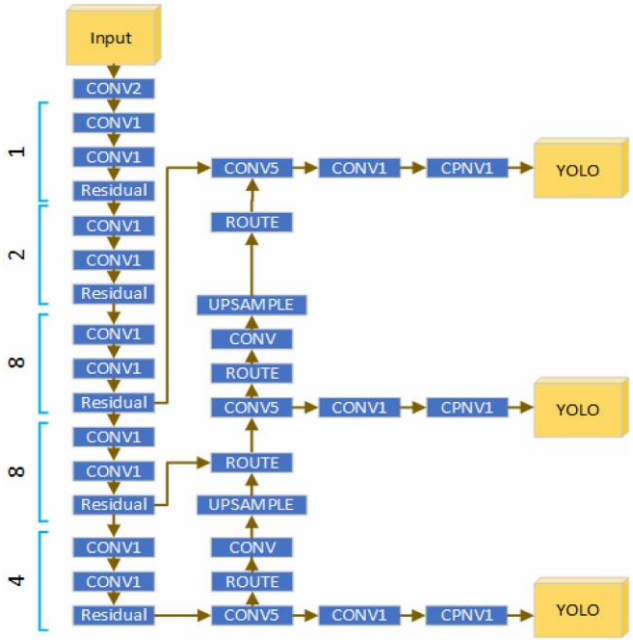

Figure 3 YOLOV3 network structure

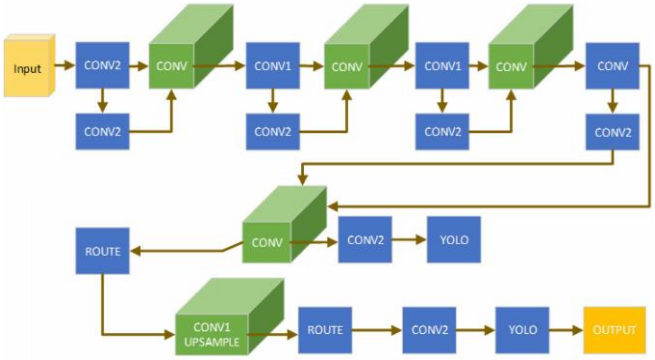

Figure 4 YOLOV3-tiny network structure

The main parameter of 2 network settings is shown in Table 1. Among them, batch represents the number of pictures sent to the network to complete an iteration when training the model. The subdivision corresponds to the number of copies of the batch. Each model is trained and packaged together to complete an iteration. The angle is the rotation angle of images, and the training data set is increased by setting the angle of the image rotation. Saturation, exposure, the hue is picture saturation, exposure, hue. The learning rate is the learning rate. Max batches is the maximum number of iterations. The policy is a learning strategy. If random is set to 1, multi-scale training is enabled.

Table 1 Network structure main parameters

Name	Parameter	Name	Parameter
Batch	64	Angle	0
Subdivisions	8	Policy	Steps
Momentum	0.9	Saturation	1.5
Decay	0.0005	Exposure	1.5
Learning Rate	0.001	Random	1
Max Batches	100000		

2.4 Weed position determination

The positioning problem of weeds position in UAV backhaul images in the world coordinate system is mainly solved by UAV image data transmission decoding and coordinate system conversion method[18]. First, obtaining the position information of the UAV and determining world coordinates of it. Second, analyzing image data of the UAV to detect weeds in the images through the network model, and output the pixel coordinates of weeds in the image. Finally, weed positions are calculated based on the relationship between the world coordinate system and the pixel coordinate system[19].

The relationship between the pixel coordinate system, the image coordinate system, and the camera coordinate system is shown in Figure 5. O_{UV} is the pixel coordinate system, O_C is the camera coordinate system, and O_W is the world coordinate system. Since the camera is fixed on the drone, the drone and the camera were assumed to have the same latitude and longitude.

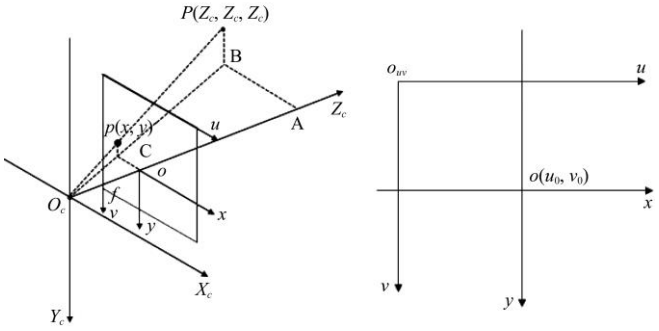

Figure 5 Relationship of camera and imaging plane

The relationship between the image plane and pixel is shown in Figure 6. The process of converting a pixel coordinate system to a world coordinate system is as follows. Take point P as an example.

(1) A point in the pixel coordinate system is turned to the image coordinate system. The pixel coordinate system and the image coordinate system are on the same plane. The midpoint of the imaging plane, that is, the intersection of the camera optical axis and the imaging plane, is the origin of the image coordinate system, the unit of it is mm, and the unit of the pixel coordinate system is pixel. The conversion of pixel coordinates and image coordinates is as shown in Equation (1), Equation (2), where d_x is the physical size of each pixel in the image plane x-direction, and y is the physical size of each pixel in the image plane y-direction.

$$x = (u - u_0)d_x \tag{1}$$

$$y = (v - v_0)d_y \tag{2}$$

(2) One point in the image coordinate system is transferred to the camera coordinate system. In Figure 5: the triangle $ABOc$ is similar to the triangle $oCOc$, and the triangle $PBOc$ is similar to the triangle $pCOc$. PB and AB can be calculated by using the following equations:

$$PB = \frac{AO_C \, pC}{oO_C} \tag{3}$$

$$AB = \frac{oCAO_C}{oO_C} \tag{4}$$

(3) One point in the camera coordinate system is transferred to the world coordinate system. When the UAV collects the image, the camera lens is facing horizontally. Therefore, regardless of the rotation of the camera around the X_W axis and Y_W, only the rotation of the camera around the Z_W is considered. As shown in Figure 6.

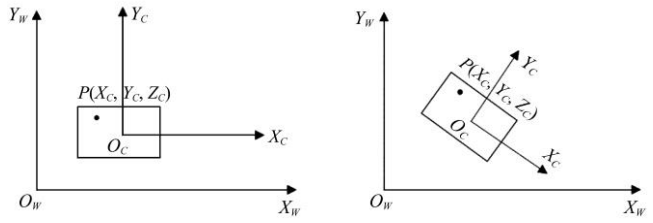

Figure 6 Relationship of camera coordinates and the world coordinates

According to the above conversion process, the relationship between the pixel and the image plane is obtained by Equation (5), the relationship between the image plane and the camera coordinate system is Equation (6), and the relationship between the camera and the world coordinate system is Equation (7). The relationship between a pixel and the world coordinate system is Equation (8). Where R is the rotation matrix and T is the offset vector.

$$\begin{bmatrix} x \\ y \\ 1 \end{bmatrix} = \begin{bmatrix} d_x & 0 & -u_0 d_x \\ 0 & d_y & -v_0 d_y \\ 0 & 0 & 1 \end{bmatrix} \begin{bmatrix} u \\ v \\ 1 \end{bmatrix} \tag{5}$$

$$Z_C \begin{bmatrix} x \\ y \\ 1 \end{bmatrix} = \begin{bmatrix} f & 0 & 0 & 0 \\ 0 & f & 0 & 0 \\ 0 & 0 & 1 & 0 \end{bmatrix} \begin{bmatrix} X_C \\ Y_C \\ Z_C \\ 1 \end{bmatrix} \tag{6}$$

$$\begin{bmatrix} X_C \\ Y_C \\ Z_C \\ 1 \end{bmatrix} = \begin{bmatrix} R & T \\ 0 & 1 \end{bmatrix} \begin{bmatrix} X_W \\ Y_W \\ Z_W \\ 1 \end{bmatrix} \tag{7}$$

$$Z_C \begin{bmatrix} x \\ y \\ 1 \end{bmatrix} = \begin{bmatrix} \dfrac{f(X_w \cos q + Y_w \sin q)}{d_x} + u_0 Z_W \\ \dfrac{f(Y_w \cos q - X_w \sin q)}{d_y} + v_0 Z_W \\ Z_W \end{bmatrix} \tag{8}$$

2.5 Data transmission

DJI cameras typically support 1280×720 (720p), 1920×1080 (1080p), 2704×1520, 3840×2160 and 4096×2160 (4K) video resolutions. The resolution determines the maximum frame rate that can be captured. The combination of resolution and frame rate can be queried directly in the SDK, but usually choosing a 4K resolution will limit the frame rate to 24/25 fps.

Developers can use the Mobile SDK to get real-time H.264 video data from Camera[20]. H.264 is a video encoding format that performs significantly better than all previous video compression standards. It is currently one of the most commonly used compression and video content distribution formats, and the decoding of H.264 data is implemented by FFmpeg. Android MediaCodec is a multimedia codec component provided by Android that Android developers can use to access the underlying multimedia.

The progress of decoding UAV image data is as follows:

(1) Receiving H.264 data sent by the UAV by initializing a NativeHelper instance object.

(2) After the mobile device receives the H.264 data, the H.264 image data was sent to the FFmpeg for parsing.

(3) After the FFmpeg decoding was completed, the image data was taken out from the FFmpeg, and the image data was buffered into the image sequence.

(4) Using Android MediaCodec as a decoder to capture keyframes in the video.

(5) After the decoding operation was completed, the image data was displayed using TextureView or SurfaceView.

(6) Stop decoding the thread and release MediaCodec and FFmpeg.

To satisfy the requirement of running the Darknet framework, the received NV21 format data was converted to a bitmap object using YuvImage.

2.6 Statistics and verification methods

The deep learning model is evaluated by precision, recall, mAP, and IOU.

Precision is used to evaluate the accuracy of the prediction, which is the number of correctly predicted positive samples divided by the total number of predicted positive samples. The recall is to evaluate the neural network's ability to discriminate positive samples. It is to correctly predict that the number of positive samples accounts for the total number of positive samples. The neural network prediction results can be divided into four types as shown in Table 2. True positive (TP) is a positive sample and it is predicted to be a positive sample; true negative (TN) is a negative sample and it is predicted to be a negative sample; A negative sample is predicted to be a positive sample; false negative (FN) is a positive sample to be predicted to a negative sample.

Table 2 Confusion matrix

	Relevant	Nonrelevant
Relevant	TP	FN
Nonrelevant	FP	TN

Precise and recall can be calculated as follows:

$$precision = \frac{TP}{TP + FP} \tag{9}$$

$$recall = \frac{TP}{TP + FN} \tag{10}$$

For multi-target detection, calculate the individual AP values for each category, and the average of these values is the mAP of the model. IOU is the degree of overlap between the actual labeled box and the network prediction box. The smaller the IOU, the farther the position between the network prediction frame and the real marker frame.

The way to verify weeds' location results is to use ground truth images. The ground truth image is a more accurate image known than the image from the test system[21]. In this study, ground live images were generated by manually selecting weeds in the experimental area.

3 Results and discussion

3.1 Weed detection results

In the experiment of this paper, the training iterated a total of 200,000 times, outputting a model every 500 iterations, so a total of 400 models were obtained.

The training results of the YOLOV3 are shown in Figure 7. When the iterations are between 0-30000, loss converges quickly; mAP rises rapidly. When the iterations are between 30000-80000, loss decreases slowly; mAP rises slowly. When the iterations are between 800-100000, the loss and mAP are stable. The

fluctuation was relatively large in the first 30,000 iterations of the IOU. After 30,000 times, the fluctuation gradually became smaller.

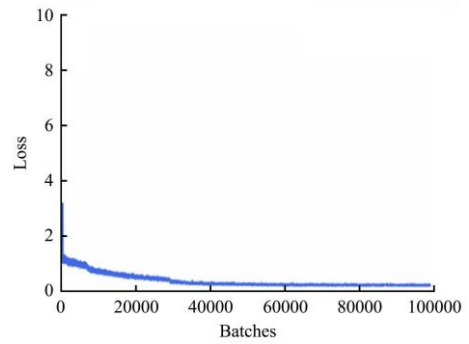

a. The loss curves

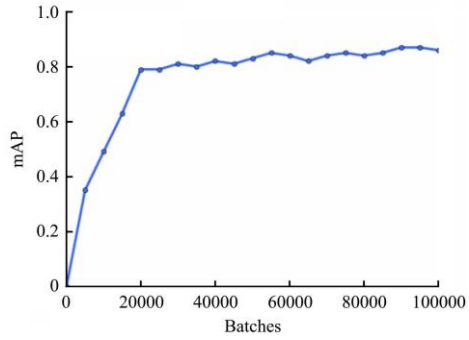

b. mAP

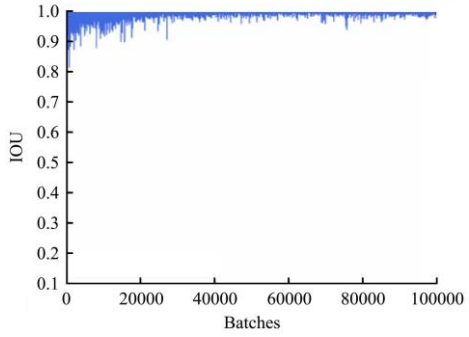

c. Avg IOU curves

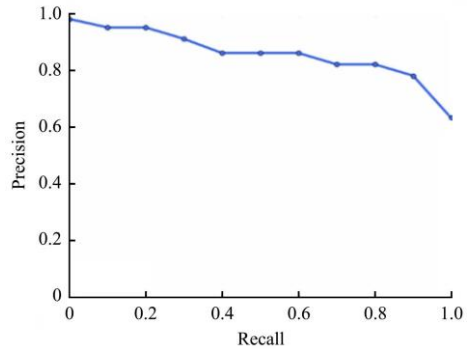

d. R-P curves

Figure 7 YOLOV3 training results

The training results of the YOLOV3-Tiny are shown in Figure 8. The loss in the number of iterations slowly decreases before the first 85000, and the 85000-100000 starts to stabilize. mAP reached its maximum at 85,000 previous iterations. IOU fluctuates throughout the training process.

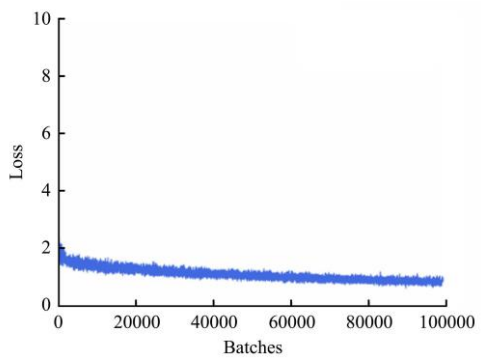

a. The loss curves

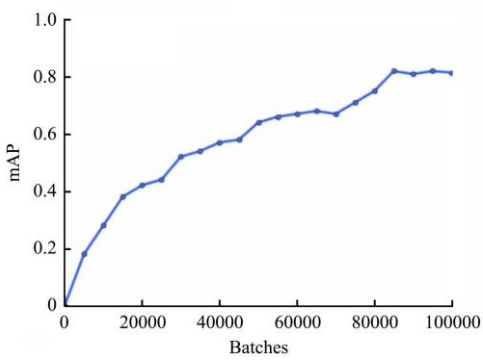

b. mAP

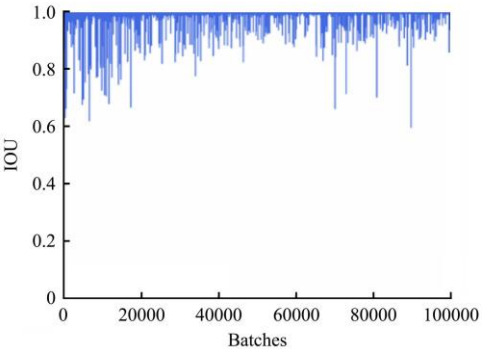

c. Avg IOU curves

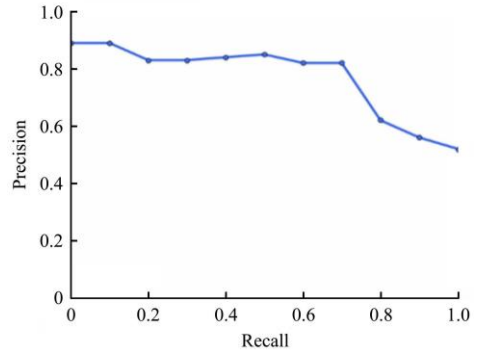

d. R-P curves

Figure 8 YOLOV3-tiny training results

The accuracy, detection speed, and size of the 2 network structures are compared. The results are shown in Table 3. The detection speed of YOLOV3-tiny is faster than YOLOV3, and the size is much smaller than YOLOV3, which is more suitable for transplantation on mobile devices. Although the accuracy of YOLOV3-tiny is lower than that of YOLOV3, to be more convenient to use in the field, this study chose the YOLOV3-tiny network as weeds recognition network.

Table 3 Performance comparison of 2 networks

	Accuracy	Speed	Size
YOLOV3	0.87%	0.08S	234MB
YOLOV3-TINY	0.78%	0.012S	33MB

Parameter values under different thresholds of YOLOV3-tiny are shown in Figure 9, select the model with the highest mAP in all models, and then use the F-Measure to select the threshold in the highest mAP model to measure the accuracy, recall rate and IOU, select a model that meets the experimental requirements.

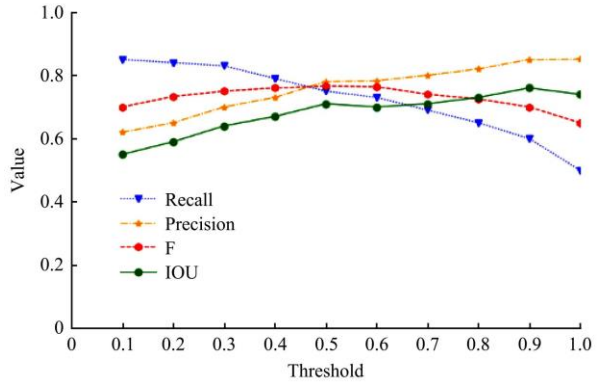

Figure 9 Parameter values under different thresholds

The final model precision was 75.2%; recall was 72.3%; mAP was 72.5% and the IOU was 70.1%. The confusion matrix of the model is shown in Tabel 4.

Table 4 Confusion matrix

	Relevant	Nonrelevant
Relevant	0.83	0.24
Nonrelevant	0.317	0.86

3.2 Weed location results

Weeds position detection is based on the deep learning target detection model, the outputs are the position and category of weeds in images, as shown in Figure 10. The Android device used in the experiment was Samsung s8 (GM-G9500, Android version 8.0.0), the real-time processing speed was 2FPS.

Figure 10 Original image and weed detection image

The detected position is based on the pixel position of the image plane. The pixel position does not provide us with effective guiding significance. Through the conversion relationship between the world coordinate system and the pixel coordinate system, the actual position of weeds in the world coordinates can be calculated. As shown in Figures 7, the latitude and longitude of weeds "GRASS_B" is (34.30617826, 108.09435262), the pixel coordinates are (2297, 2549), the latitude and longitude of weeds "GRASS_D" are (34.30615961, 108.09434738). The pixel coordinates are (2821, 681). The latitude and longitude of "GRASS_B" calculated by Equation (8) are (34.30617855, 108.09435236), and the coordinates of "GRASS_D" (34.30615945, 108.09434762). In this way, 10 images of 10 weeds were randomly selected for measurement. The measurement results are shown in Figure 11. The distance from each point to origin represents the value of each error. Error is distributed between 0~20 cm, the average error is 10.314 cm.

3.3 Weeding prescription map

Based on the spatial distribution of weeds, a prescription map of field spraying herbicides is drawn. The spraying amount is classified according to the number of weeds per square meter. The prescription map is shown in Figure 12.

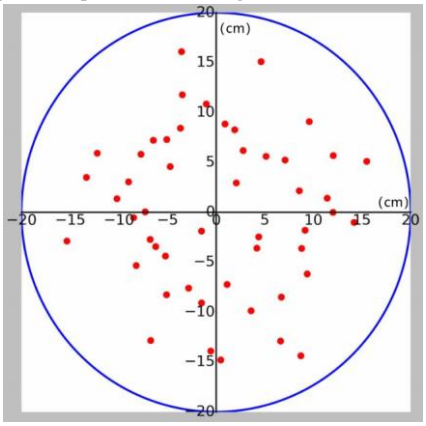

Figure 11 Distribution of errors

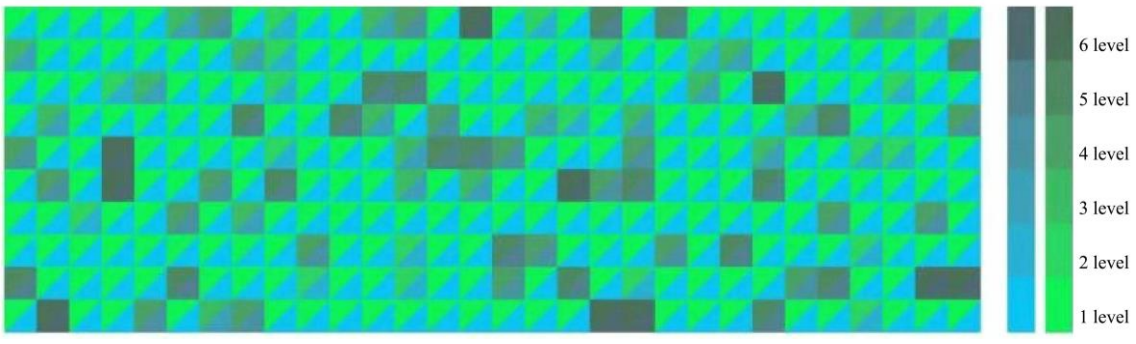

Figure 12 Prescription map of field

4 Conclusions

In this study, a real-time detection system for field weeds based on UAVs and mobile devices was designed to verify the feasibility of detecting weeds in real time. This system mainly supports plant protection spray UAVs. The results of this study are of great significance in achieving precise spraying. For the overall study, the following conclusions can be drawn:

(1) Weeds in crop field can be detected in real time through a network model. The target detection function uses the YOLOV3-tiny network structure training model to find the optimal model by comparing mAP, and quickly realize weeds recognition under the premise of ensuring the accuracy of detection. According to the specific requirements, the data set can be adjusted for different types of weeds detection, which has wide applicability.

(2) A UAV flight path by setting a working area was created to accurately divide working area. Firstly, the latitude and longitude of the UAV under the WGS-84 coordinate system were transferred to the latitude and longitude of the GCJ-02 coordinate system so that the UAV could correctly display position on map. The route and waypoint were generated according to the operator's defined working areas and overlap rate. Finally, all the waypoints were uploaded to navigate the UAV fly according to waypoints.

(3) The GPS positioning function can effectively locate weeds in crop field. Through the position information of the UAV and weeds position in the image, the similar triangle method is used to calculate position of weeds in the world coordinate system, which provides support for subsequent crop spray application process, which can save pesticide, water and time.

(4) A prescription map of field spraying herbicides was drawn based on the number of weeds per square meter, which can be used to support weeding operations.

Acknowledgments

This work was funded by the National Key R&D Program of China (2018YFD0200402) and Fundamental Research Funds for the Central Universities (No.2452019028).

[References]

[1] Brown R, Steckler J-P, Anderson G. Remote sensing for identification of weeds in no-till corn. Transactions of the ASAE, 1994; 37(1): 297–302. doi: 10.13031/2013.28084.

[2] Gerhards R, Sökefeld M, Timmermann C, et al. Site-specific weed control in maize, sugar beet, winter wheat, and winter barley. Precision Agriculture, 2002; 3(1): 25–35. doi: 10.1023/A:1013370019448.

[3] Vrindts E, De Baerdemaeker J, Ramon H. Weed detection using canopy reflection. Precision Agriculture, 2002; 3(1): 63–80. doi: 10.1023/A:1013326304427.

[4] Slaughter D, Giles D K, Downey D. Autonomous robotic weed control systems: A review. Computers and Electronics in Agriculture, 2008; 61(1): 63–78. doi: 10.1016/j.compag.2007.05.008.

[5] López‐Granados F. Weed detection for site‐specific weed management: mapping and real‐time approaches. Weed Research, 2011; 51(1): 1–11. doi: 10.1111/j.1365-3180.2010.00829.x.

[6] Steen K A, Christiansen P, Karstoft H, et al. Using deep learning to challenge safety standard for highly autonomous machines in agriculture. Journal of Imaging, 2016; 2(1): 6. doi: 10.3390/jimaging2010006.

[7] Kamilaris A, Prenafeta-Boldú F X. Deep learning in agriculture: A survey. Computers and Electronics in Agriculture, 2018; 147:70–90. doi: 10.1016/j.compag.2018.02.016.

[8] Carrio A, Sampedro C, Rodriguez-Ramos A, et al. A review of deep learning methods and applications for unmanned aerial vehicles. Journal of Sensors, 2017; 2017: 1–13. doi: 10.1155/2017/3296874.

[9] Milioto A, Lottes P, Stachniss C. Real-time semantic segmentation of crop and weed for precision agriculture robots leveraging background knowledge in CNNs.2018 IEEE International Conference on Robotics and Automation (ICRA). IEEE, 2018: 2229–2235. doi: 10.1109/ICRA.2018.8460962.

[10] Potena C, Nardi D, Pretto A. Fast and accurate crop and weed identification with summarized train sets for precision agriculture. Advances in Intelligent Systems and Computing, 2017; 105–121. doi: 10.1007/978-3-319-48036-7_9.

[11] Howard A G, Zhu M, Chen B, et al. Mobilenets: Efficient convolutional neural networks for mobile vision applications. ArXiv, 2017; Available:http://arxiv.org/abs/1704.04861 Accessed on [2020-03-11]

[12] Zhang X, Zhou X, Lin M, et al. Shufflenet: An extremely efficient convolutional neural network for mobile devices; proceedings of the Proceedings of the IEEE Conference on Computer Vision and Pattern Recognition, F, 2018 ; 6848–6856. doi: 10.1109/CVPR.2018.00716.

[13] Wang R J, Li X, Ling C X. Pelee: A real-time object detection system on mobile device. Advances in Neural Information Processing Systems, 2018; 1963–1972.

[14] Redmon J , Divvala S , Girshick R , et al. You Only Look Once: Unified, Real-Time Object Detection. 2016 IEEE Conference on Computer Vision and Pattern Recognition (CVPR). IEEE, 2016. doi: 10.1109/CVPR.2016.91.

[15] Redmon J, Farhadi A. YOLO9000: better, faster, stronger. Proceedings of the IEEE conference on computer vision and pattern recognition, 2017; 7263–7271. doi: 10.1109/cvpr.2017.690.

[16] Redmon J, Farhadi A. YOLOV3: An incremental improvement. arXiv preprint arXiv:180402767, 2018;

[17] Redmon J. Darknet: Open source neural networks in c. http://pjreddiecom/darknet/. Accessed on [2020-03-11].

[18] Juan D. Understanding of Object Detection Based on CNN Family and YOLO. Journal of Physics: Conference Series, 2018; 1004(1): 012029. doi: 10.1088/1742-6596/1004/1/012029.

[19] Sheikh Y, Khan S, Shah M, et al. Geodetic alignment of aerial video frames. Video Registration. Springer, 2003; 144–79. doi: 10.1007/978-1-4615-0459-7_7.

[20] Wiegand T, Sullivan G J, Bjontegaard G, et al. Overview of the H. 264/AVC video coding standard. IEEE Transactions on Circuits and Systems for Video Technology, 2003; 13(7): 560–76. doi: 10.1109/tcsvt.2003.815165.

[21] Barrero O, Perdomo S A. RGB and multispectral UAV image fusion for Gramineae weed detection in rice fields. Precision Agriculture, 2018; 19(5): 809–22. doi: 10.1007/s11119-017-9558-x.